Interactions of lipid monolayers with the natural biopolymer hyaluronic acid

R. Ionov[a,b,*], A. El-Abed[a], M. Goldmann[c], P. Peretti[a]

[a]LNPC, Université René Descartes, 45, rue des Saints Pères, 75270 Paris Cedex 06, France
[b]College of Sciences «Leonardo da Vinci» PO Box 946, BG-1000 Sofia, Bulgaria
[c]LURE, Université Paris Sud, 91405 ORSAY France

Abstract

The interaction of the natural mucopolysaccharide hyaluronic acid with different lipids, present in the natural membranes, was studied at the lipid/water interface using thermodynamic methods and X-ray diffraction. The results show that this biopolymer modifies the properties and the structure of the lipid monolayer. The two-dimensional crystalline lattice and domain structure of the charged octadecylamine monolayer are strongly disturbed by the hyaluronic acid, the monolayer compressibility increases and the monolayer collapse pressure drops down. In addition, the presence of charged lipid interfaces influences the structural organisation of the hyaluronic acid at the membrane/water interfaces. The impacts of these results on the structural organisation at the membrane interface are discussed.
© 2004 Elsevier B.V. All rights reserved.

Keywords: Membrane; Lipid monolayer; Hyaluronic acid; Biopolymer; Grazing angle X-ray diffraction; Flourescence microscopy; Adsorption; Surface presure isotherm

1. Introduction

Lipids are the major component constituting the biological membranes. The state of the membrane depends on the physico-chemical characteristics of both the lipids and the membrane bond proteins. This state could be influenced by the interaction of the lipids and the membrane proteins with the active biopolymers present at the membrane/water interface (e.g., hyaluronic acid, collagen).

Hyaluronic acid is a natural high molecular weight unbranched polysaccharide found throughout connective tissues. In some tissues, like vitreous humour, synovial fluid, it is the primary component responsible for the function and the physical characteristics associated with these substances [1–4]. In other tissues such as skin,

cartilage and aorta, it is found as a minority component which acts as a stabilising and organising agent on the structure of some proteins [1]. Hyaluronic acid (HYA) and its derivatives are broadly used in pharmacy and medicine, especially in segment surgery, wound and burn therapy, drug matrices, and HIV-antibody [5–8]. Many of the functions of the hyaluronic acid are related to its physico-chemical, structural properties and its interactions with membrane lipids [9–13]. For example, the vitreous humour is constituted from 99% water and 1% mixture of collagen and hyaluronic acid. HYA is an active pH-dependent biopolymer, which may influence the state of the neighbour Burch membrane. In concentrated solutions, due to the hydrogen bonds, various conformations of this mucopolysaccharide are probable—from double helices to compact states of densely packed chains [1,14–18]. The questions that remain open are: How does this important biopolymer interact with the membranes? Does it influence the structural organisation of membrane lipids? How important is the effect of the negative charge of HYA? Does its

---

* Corresponding author. LDSMM, Université de Lille 1, UFR de Physique, Bat. P5, 59 655 Villeneuve d'Ascq Cedex, France. Tel.: +33 3 2033 6391; fax: +33 3 2043 6857.
E-mail address: r_ionov@hotmail.com (R. Ionov).

structural conformation at the lipid/water interface differ from the bulk state?

To answer some of these questions, we performed surface studies of the hyaluronic acid activity at the air/water and lipid/water interfaces. Langmuir monolayers are suitable systems to study the structural organisation of the lipid monolayers and the interactions at the lipid/water interface [19–26]. We studied thermodynamically and structurally the influence of the hyaluronic acid on the lipid monolayers as well as the adsorption kinetics of this biopolymer at various interfaces. The most essential structural modification is obtained with positively charged octadecylamine monolayers. They are analysed in detail because of their relevance to the biological membranes where the charged alkanes appear as a consequence of the lipids metabolism.

2. Experimental

Hyaluronic acid (HYA) sodium salt from bovine tracheae was a Fluka product with mean molecular weight of about 80 000. The lipids 1,2-dipalmitoyl-sn-glycero-3-phosphatidylcholine (DPPC), 1,2-myristoyl-sn-glycero-3-phosphatidylethanolamine (DMPE), 1,2-dipalmitoyl-sn-glycero-3-phosphatidylglycerol (DPPG), 1,2-dipalmitoyl-sn-glicero-3-[phospho-L-serine) sodium salt (DPPS) and octadecylamine (ODA)) were supplied by Avanti Polar Lipids (Alabama) and Sigma-Aldrich (France). The salts and solvents were high-purity Merck, Fluka, Prolabo, and Sigma products. The physiological aqueous solution contained 0.1 M NaCl of pH 7.0, which was adjusted by means of 1×10^{-3} M

phosphate buffer (Na_2HPO_4/NaH_2PO_4 of 1:1 molar ratio, p.a. grade, Merck). pH was varied by means of 0.1 M NaOH water solutions. Experiments with pure water, $NaHCO_3$ aqueous subphase and 10^{-3} M $CaCl_2$ were performed as well. Deionized pure water of resistivity 1.8×10^7 Ω/cm was used (ELGA filter system). The temperature of the subphase was 20 °C.

The adsorption was performed by injection of 10^{-3} M water solutions of hyaluronic acid under the pure air/water interface or under lipid/water interface.

Fig. 2. Adsorption kinetics of HYA at different concentrations: (1) 1.25×10^{-6} M; (2) 7.14×10^{-7} M; (3) 2.38×10^{-7} M; (4) 1.90×10^{-7} M.
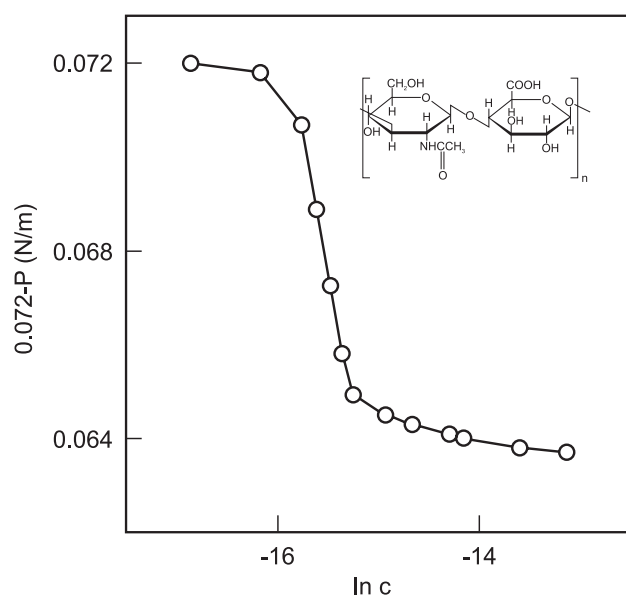

Fig. 1. Adsorption isotherm (surface tension versus concentration (M/L)) of HYA at the air/water interface at 20 °C. The inset shows HYA structure. P is the surface pressure.
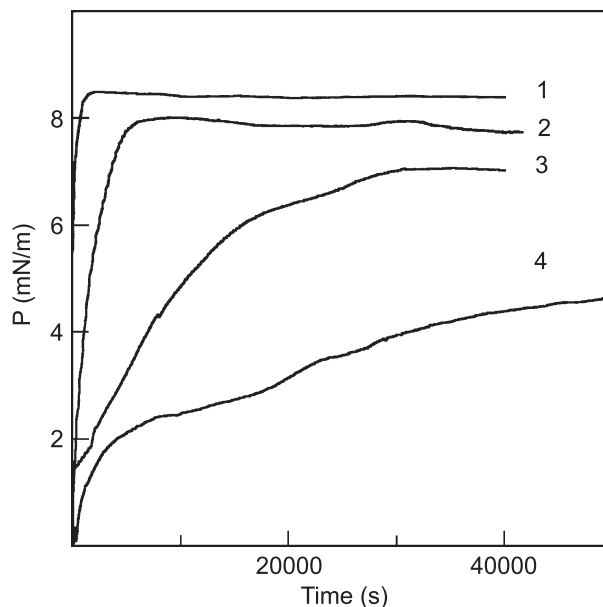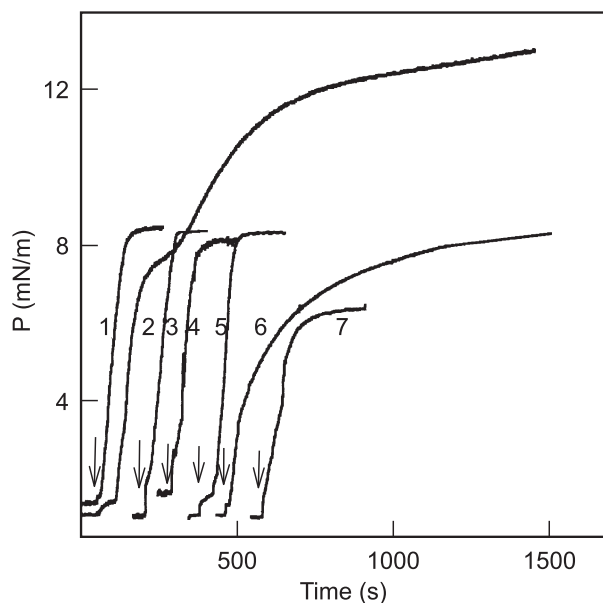

Fig. 3. Adsorption kinetics of HYA injected under the lipid monolayers compressed to about 1 mN/m: (1) DPPC; (2) ODA; (3) DPPS; (4) DPPS+Ca^{2+}; (5) DMPE; (6) DPPG; (7) DPPG+Ca^{2+}. HYA concentration is 1.25×10^{-6} M and pH=7. The arrows indicate the moment of injection of HYA.

Table 1
Surface pressure relaxation times of HYA injected under different lipid monolayers compressed to about 1 mN/m

DPPG	DPPG+Ca^{2+}	DPPS	DPPS+Ca^{2+}	DMPE	DPPC	ODA
219 s	71 s	49 s	37 s	31 s	36 s	47/380 s

The standard error is about 1%.

An automatically controlled Langmuir trough [19,25] was used to study the lipid monolayers. Surface pressure was measured by means of the Wilhelmy plate method with precision of about 0.1 mN/m. The monolayer compression speed was about 0.01 nm^2/molec. min. The temperature region of the trough operation was from 0° to 70°.

Synchrotron X-ray diffraction experiments from lipid monolayers were performed at LURE, Orsay, France using the experimental equipment [27] at the beam line D41B. Fluorescence microscopy experiments were performed using Olympus imaging system and intensified AIS camera. Molecular probe phospholipid NBD day marker N-3787 at lipid/day molar ratios of about 1:800 was used.
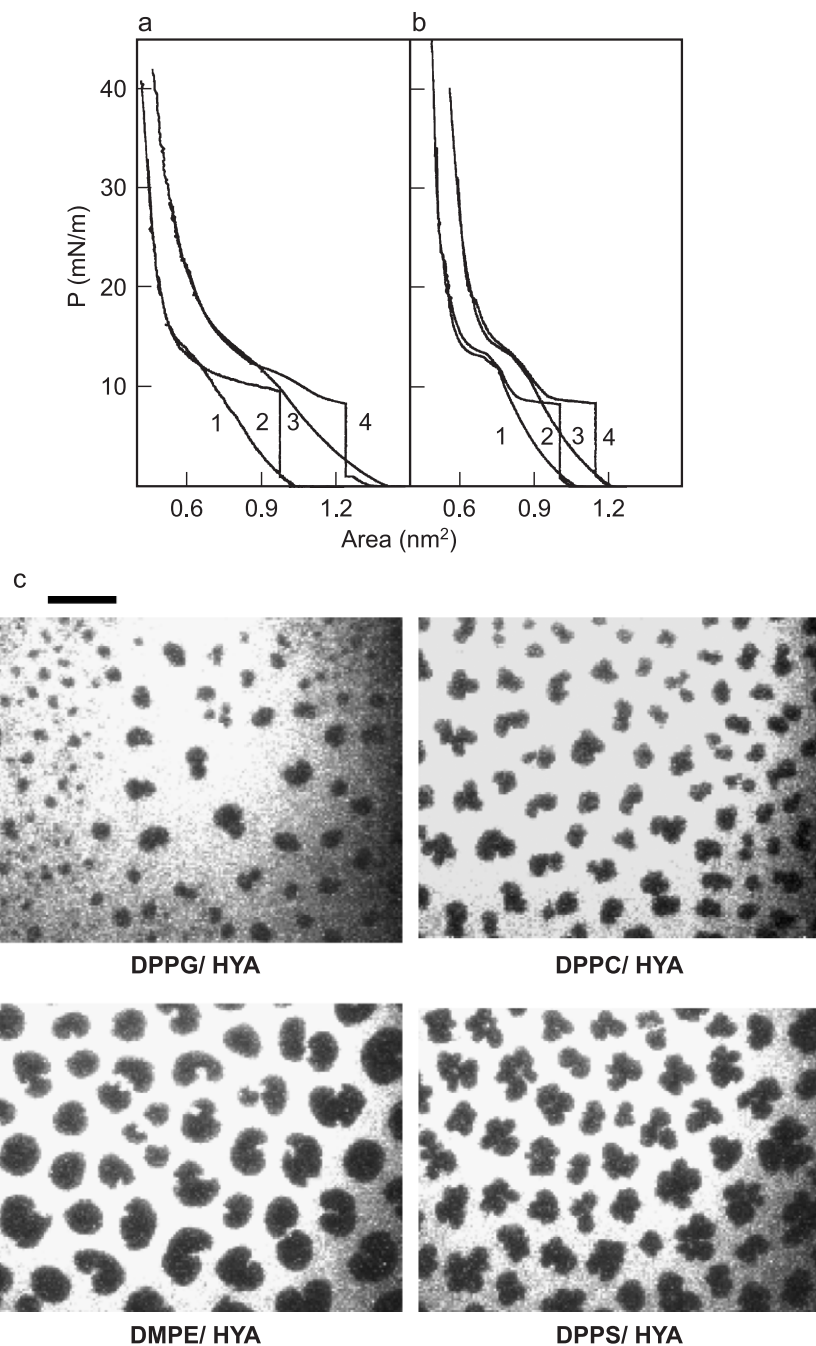

Fig. 4. Comparison of surface pressure isotherms of (a) 1—DPPS; 2—DPPS+HYA; 3—DPPG; 4—DPPG+HYA; (b) 1—DMPE; 2—DMPE+HYA; 3—DPPC; 4—DPPC+HYA. HYA concentration is 1.25×10^{-6} M and pH=7. (c) Images of 2D phospholipid domains in the presence of HYA: DPPG/HYA—15 mN/, 20°; DPPC/HYA—13 mN/m, 27°; DMPE/HYA—15.7 mN/m, 27°; DPPS/HYA—11 mN/m, 37°. The bar corresponds to about 50 μm.

The adsorption kinetics was analysed using nonlinear least square fit procedure of the Origin software (Microcal, USA).

3. Results

The adsorption isotherm of the hyaluronic acid at the air/water interface shows an equilibrium surface pressure (ESP) value of about 8.2 mN/m at volume concentrations of about 1×10^{-6} M (Fig. 1).

The time dependence of the adsorption of the hyaluronic acid at the air/water interface is shown in Fig. 2. The relaxation times depend on the biopolymer subphase concentration, and vary to about two orders of magnitude. At low concentrations (1×10^{-7} M), the relaxation time is about 4 h and at concentrations higher than 1×10^{-6} M the relaxation time is about 180 s. The adsorption of the hyaluronic acid with a bulk concentration of about 1.2×10^{-6} M under various lipid monolayers compressed to 1 mN/m shows different relaxation times (Fig. 3) varying from 380 to 31 s (Table 1). The values of the steady-state pressure depend on the hyaluronic acid lipid interactions and vary from 7.6 to about 22 mN/m. With Ca^{2+} ions in the subphase, the relaxation process was faster for negatively charged lipids (DPPG and DPPS). Two relaxation times of 47 and 380 s were estimated for the primary faster adsorption process at the ODA/water interface and for the secondary process of ODA–HYA monolayer rearrangement, respectively.

The surface pressure isotherms of some phospholipids, present in the natural cell membranes, and the effect of HYA at physiological conditions are shown in Fig. 4a and b. The hyaluronic acid was injected in the subphase under phospholipid monolayers compressed to about 1 mN/m. Due to the surface activity of hyaluronic acid, the pressure rises to its steady-state value of about 8.2 mN/m as shown in Fig. 2. Thereafter, the film was compressed. The isotherms at higher surface pressure values coincide with those of the pure phospholipids in absence of hyaluronic acid. The two-dimensional phospholipid domains observed by means of fluorescence microscopy in the presence of hyaluronic acid are shown in Fig. 2c. The 2D domain shape of these phospholipids was not essentially influenced by HYA but the mean domain size was about 10% lower.

The isotherms of the positively charged ODA monolayers are strongly modified by the presence of hyaluronic acid (Fig. 5). The pure ODA monolayer isotherm shows two distinct regions and a kink at about 20 mN/m. The biopolymer was injected in the subphase under the ODA
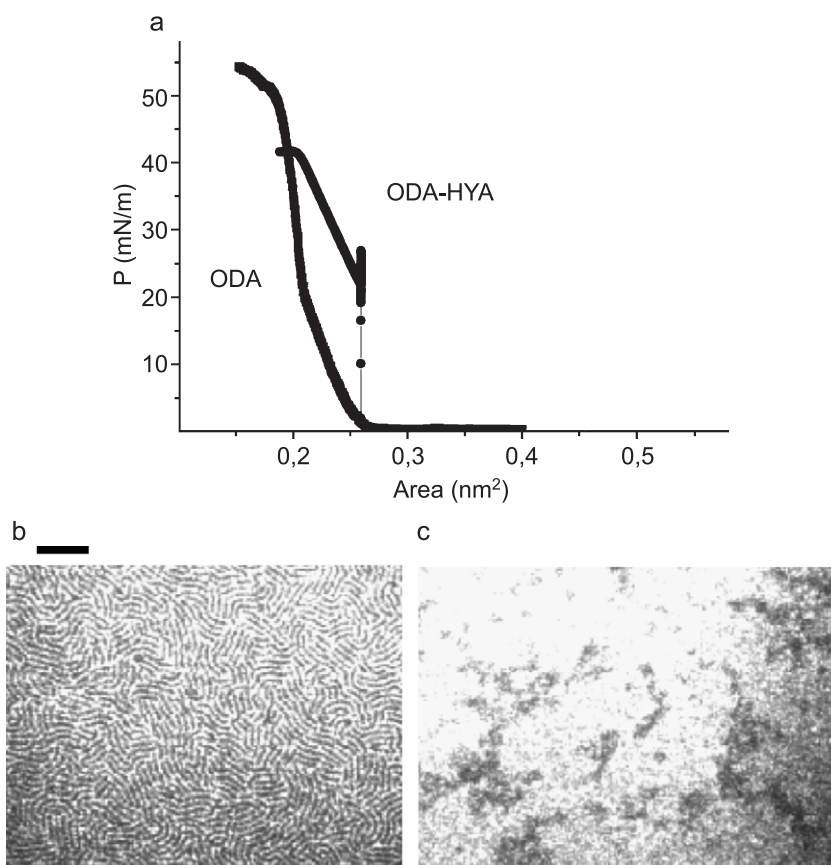

Fig. 5. (a) Comparison of surface pressure isotherms of ODA and ODA+HYA monolayers. (b) Image of 2D ODA domains at about 10 mN/m; (c) image of 2D ODA–HYA monolayer at about 15 mN/m. HYA concentration in the aqueous subphase is 1.25×10^{-6} M and pH=7. The bar corresponds to 50 μm.

lipid monolayers, which was compressed to about 1 mN/m. The surface pressure rises initially to about 27 mN/m and thereafter stabilises within 3 h at about 22 mN/m. The ODA molecular areas of 0.203 and 0.220 nm^2 at 30 mN/m were observed without and in the presence of hyaluronic acid in the aqueous subphase, respectively. The same increase of about 0.017 nm^2 of the molecular area was measured when HYA was injected under the ODA monolayer compressed to 30 mN/m at constant pressure and temperature. Without hyaluronic acid in the subphase, the monolayers of ODA were not very stable and they showed slow reduction of the surface area at constant surface pressure within a time scale of about 3 h. In the presence of the hyaluronic acid, the monolayers become very stable and the surface area remained constant for the entire observation period of about 72 h. The collapse pressures of pure ODA and ODA–HYA monolayers are 50 and 41 mN/m, respectively.

Two-dimensional ODA domains were observed within the surface pressure region from 1.5 to 12 mN/m by means of fluorescence microscopy. Well-defined arrays of rod-like two-dimensional domains were obtained (Fig. 5b) at surface pressure of about 10 mN/m. The mean length of the domains is about 25 mm and the mean width is about 3.5 mm. Within the surface pressure region from 12 to about 20 mN/m the monolayer shows homogeneous morphology. At higher pressures, domains were not observed.

The ODA monolayer was decompressed and recompressed to about 1 mN/m and HYA was injected in the water subphase to a concentration of about 1×10^{-6} M. The presence of hyaluronic acid modifies the surface morphology of the monolayer and nonuniform domain structures were observed (Fig. 5c).

Fig. 6a shows the variation of the X-ray diffraction patterns for ODA monolayers at pure air/water interface. The main peak position in Q vector space is at about 15.207 nm^{-1} at 30 mN/m, which corresponds to a Bragg spacing of about d=0.4130±0.0002 nm. The position of the peak varies from 14.695 to 15.215 nm^{-1} and its full width at half maximum (FWHM) varies from 0.0024 to 0.0021 nm^{-1} for surface pressure variation from 6 to 40 mN/m, respectively. The inset in Fig. 6a shows the rod scan of the planar peak at 40 mN/m.

In the presence of hyaluronic acid, the peaks of ODA monolayers are broader (Fig. 6b). With the increase of the surface pressure, the peak position shifts slightly toward lower wave vectors Q. Within the time scale of about 12 h, the intensity of the main peak drops down and a new broad shoulder at about 0.4584 nm appears at a surface pressure of about 30 mN/m.
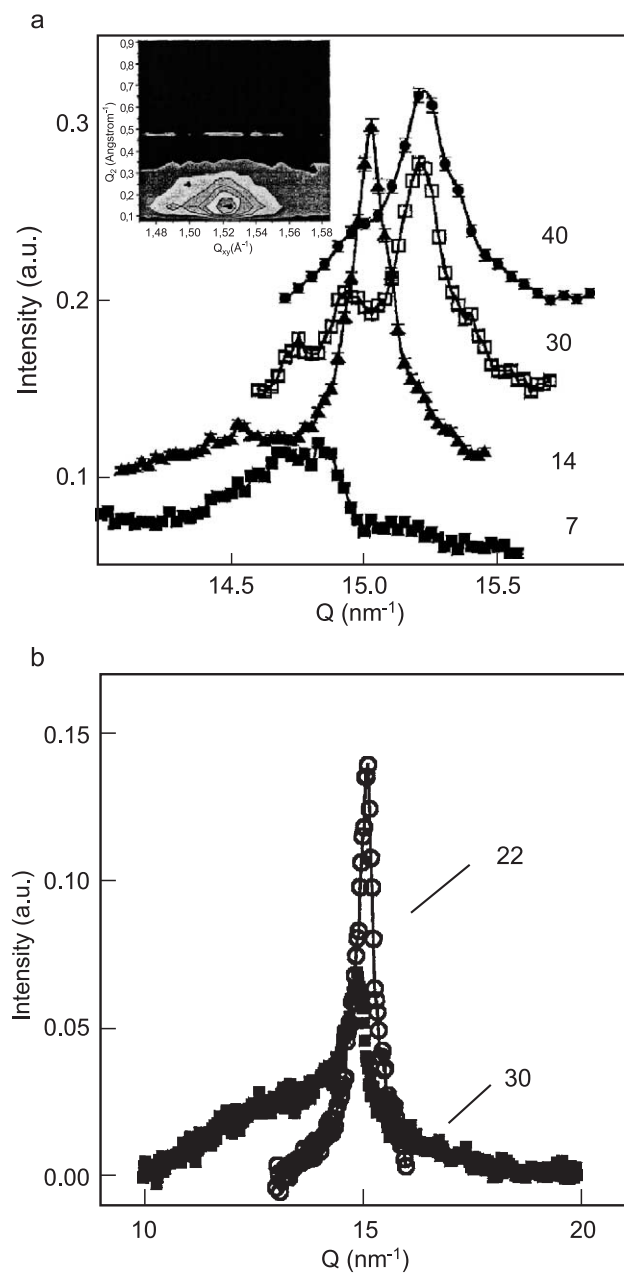
4. Discussion

The surface activity of the water-soluble biopolymer HYA plays an important role at the membrane/water interface and it may modify the membrane properties. Using the Gibbs equation for surface pressure variation

$$d\pi = \frac{kT}{A} \, d\ln c$$

(where k is the Boltzmann constant, T is the absolute temperature, A is surface molecular area, and c is the biopolymer activity, considered equal to the bulk concentration, provided it is sufficiently low), a molecular area of about 9.92 nm^2 can be determined for the adsorbed hyaluronic acid at the air/water interface (Fig. 1).

Detailed structural investigations have determined a large variety of HYA structural packings, which depend on

Fig. 6. X-ray diffraction patterns from (a) pure ODA monolayer and (b) HYA monolayer at different surface pressures. Q is the wave vector. The numbers indicate the surface pressure. The inset in (a) shows the rod scan at 40 mN/m.

temperature, humidity and pH [4,14,16]. In particular, HYA may show: (i) a "random coil" structure in the bulk state, in dilute aqueous solutions at neutral pH; (ii) tetragonal packing of double helices at acidic pHs with a helix pitch of about 3.3 nm composed of four disaccharide units, and interduplex distance of about 1.7 nm; (iii) orthorhombic or tetragonal packing of single helices strands with helix pitch of about 3.4 nm and four disaccharide units per pitch with interstrand distance of about 0.99 nm at neutral pH. This means that the average rise per disaccharide unit is about 0.85 nm and the area occupied per disaccharide unit is about 0.84 nm^2.

One may expect that the HYA arrangement at the interface could be close to the known HYA structures of "random coil" or single helices strands. The mean number of monomers of the HYA biopolymer used in our study is about 206. Therefore, one could speculate that each HYA molecule exposes at the air/water interface about 12 (9.92/0.84) disaccharide units (Fig. 1, inset). This means (206/12 ≈ 17) that about one unit of each fourth pitch (4×4) exposes its methylene group at the interface. This speculation shows reasonable values with the helical structure of HYA and indicates that this structure may be one probable arrangement of HYA at the interface. The "random coil" HYA organisation at the interface with 12 disaccharide units in contact with the interface could be another possible HYA arrangement.

The adsorption kinetics of the water soluble HYA acid at the air/water interface could be described in terms of first order equation [28]:

$$\pi_t = \pi_s - (\pi_s - \pi_o) \exp(-t/\tau),$$

where τ is the relaxation time, π_o, π_t and π_s are the surface pressures at time $t=0$, t and steady-state conditions. This process is determined by the balance between the adsorption/desorption events, molecular rearrangements and structure at the interface. At low concentrations of HYA, the role of desorption is important. At higher concentrations, the desorption flux is lower because of higher probability of hydrogen bond formation and molecular reorganisation. This process determines shorter relaxation times of about 180 s.

The lowest relaxation time values (Table 1) are determined for adsorption of HYA under neutral zwitterionic phospholipids (DPPC, DMPE). The presence of phospholipids at the interface creates possibilities for formation of hydrogen bond bridges of HYA with phospholipid head groups, which reduces the desorption flux and finally the relaxation process at interface is faster. The electrostatic repulsion between negatively charged HYA and DPPG monolayer creates an additional barrier, which increases the relaxation time. This process could be controlled by the presence of Ca^{2+} ions (Fig. 2, Table 1).

The adsorption of HYA under positively charged ODA monolayers shows two relaxation processes. The faster one is related to reduced role of the desorption process and the slowest one is due to the structural reorganisation because of the attractive HYA–ODA electrostatic interactions. The behaviour of this monolayer will be discussed below.

The relaxation times show that the adsorption of HYA at the lipid/water interface is much faster and differs from the relaxation process at the pure air/water interface. It depends on the charge, the hydrogen bonding capability of the lipid head groups and on the presence of ions in the aqueous subphase.

The weak interaction of HYA with phospholipid head groups influences the relaxation process and slightly the size of the two-dimensional lipid domains formed at the air/water interface (Fig. 4). The isotherms and the domain shape remain unchanged, which may suggest that the lipid monolayer structural arrangement does not change.

The interaction of negatively charged HYA biopolymer with positively charged ODA is much stronger, which results in an essentially new HYA–ODA monolayer behaviour.

4.1. Pure ODA monolayers

The ODA monolayers are in a fully hydrated and charged state at pH 7 while they exist in uncharged state at pH 10 [29,30]. The ESP of ODA monolayers is about 18.2 mN/m and the monolayer collapse is at about 50 mN/m. A transition region from 1.5 to about 12 mN/m was found by the fluorescence microscopy. The elongated shape of ODA 2D domains observed within the transition region (Fig. 5b) is a typical indication of the dominating role of the electrostatic interactions [31,32]. The isotherm (Fig. 5a) shows after the transition region a liquid condensed phase (LC) up to 22 mN/m with compressibility of about 9.5 m/N (at 16 mN/m), and at higher pressures a solid state with a compressibility coefficient of about 2.8 m/N (at 30 mN/m). The transition region is a nonideal first order transition which is difficult to be distinguished directly from the monolayer isotherm. Within the transition region at 6 mN/m, the X-ray diffraction shows (Fig. 6) the coexistence of two LC phases: a first phase with rectangular lattice parameters $a=0.504$ nm and $b=0.414$ nm and a second hexagonal phase with lattice parameter $a=0.488$ nm. Both phases are tilted to about 5° (deduced from the rod scans). Within the LC phase region dominates the second untilted hexagonal structural arrangement with $a=0.483$ nm and its correlation length is about 12 nm at 14 mN/m. At 30 mN/m the hexagonal arrangement coexists with a nontilted rectangular phase, which becomes dominating at 40 mN/m and which has the following lattice parameters: $a=0.484$ nm and $b=0.409$ nm.

4.2. ODA–HYA monolayers

The adsorption of HYA under the ODA monolayer modifies the properties of this monolayer. The stability of the ODA–HYA monolayer increases substantially, the phase transition region and the regular domain structure disappear. The monolayer compressibility increases significantly to a value of about 11.5 m/N. The monolayer collapse pressure

drops down to about 41 mN/m, because of a reduction of the ODA head group lateral repulsion. This is a result of an increase in the intermolecular distance and electrostatic interactions with HYA. The comparison of the ODA and ODA–HYA monolayer isotherms (Fig. 5a) shows that the second relaxation process of HYA–ODA system in the adsorption curve (Fig. 2) occurs within the ODA monolayer LC phase region. The obtained steady-state adsorption pressure of about 22 mN/m corresponds to both the end of the LC_2 phase transition region and the ESP value of ODA monolayers. The ODA–HYA monolayers show higher molecular areas. The molecular area increase of about 0.017 nm^2 at 30 mN/m for isohore-isothermal expansion of the monolayer corresponds to a variation of the free energy of about 3.19 meV. This energy is associated with the new structural organisation of ODA–HYA monolayer induced by the additional electrostatic interactions and which is spent by the ODA–HYA monolayer against the external lateral forces.

Analysis of the X-ray diffraction pattern from ODA–HYA monolayers (Fig. 6b) shows untilted aliphatic chains at the air/water interface which arrange in a hexagonal structure with parameter a=0.481 nm (at 22 mN/m). The correlation length is about 8 nm. The drop down of the intensity and the shift of the peak position toward lower values of Q with the increase of the surface pressure indicate that the disorder of the lipid chains and the lattice parameters increase. The data of long-term relaxed ODA–HYA monolayer show that the pure ODA monolayer structural arrangement is disturbed. The new ODA–HYA monolayer structural arrangement results in: (i) appearance of a new broad shoulder in the X-ray diffraction pattern, (ii) drop down of the intensity of the main ODA peak, (iii) higher monolayer compressibility of about 11.5 m/N determined at 30 mN/m, and (iv) lower collapse pressure of the monolayer at 41mN/m related to the electrostatic interactions of ODA with HYA. The additional peak (shoulder) originates from a monolayer thickness of about 0.4 nm (deduced from the rod scans), which fits with the HYA structural parameters. The appearance of only one peak originating from HYA packing does not allow to define the exact HYA structure. However, the presence of this peak at the charged ODA monolayer/water interface and the absence of an X-ray diffraction peak at the uncharged or the monolayer free air/water interface show that HYA adopts a well-defined structure at the positively charged interface. The lipids composing the biological membranes have lateral monolayer mobility and some of them possess positive charges. The minimisation of the interfacial electrostatic energy of the lipid–HYA system composed of nonstatic positive and negative charges will result in a lateral lipid redistribution and a new defined structural organisation of HYA at the membrane interface.

The obtained results have an important biomedical impact. They show that HYA is an active biopolymer which

is able to modify the membrane structure. In turn, the presence of the charged membrane will induce a specific organisation of this biopolymer at the membrane/water interface that may in turn influence the membrane transport properties.

References

[1] I. Dea, R. Moorhouse, D. Rees, S. Arnott, J. Guss, E. Balazs, Hyaluronic acid: a novel, double helical molecule, Science 179 (1973) 560–562.

[2] M. Flowers, R. Marlowe, S. Lee, N. Lavalle, A. Rupprecht, Optical and physical properties of wet-spin films of Na hyaluronate, Biophys. J. 63 (1992) 323–326.

[3] A. Shard, M. Davies, S. Tendler, L. Benedetti, M. Purbrick, A. Paul, G. Beamson, X-ray photoelectron spectroscopy and time of flight SIMS investigations of hyaluronic acid derivatives, Langmuir 13 (1997) 2808–2814.

[4] S. Arnott, A. Mitra, S. Raghunathan, Hyaluronic acid double helix, J. Mol. Biol. 169 (1983) 861–872.

[5] L. Hume, H. Lee, L. Benedetti, Y. Sanzgiri, E. Topp, V. Stella, Ocular sustained delivery of prednisolone using hyaluronic acid benzyl ester films, Int. J. Pharm. 111 (1994) 295–298.

[6] J. Zheng, Y. Ito, Y. Imanishi, Cell growth on immobilized cell-growth factor: 10. Insulin and polyallylamine co-immobilized materials, Biomaterials 15 (1994) 963–968.

[7] L. Ruiz-Cardona, Y. Sanzgiri, L. Benedetti, V. Stella, E. Topp, Application of benzyl hyaluronate membranes as potential wound dressing: evaluation of water vapour and gas permeabilities, Biomaterials 17 (1996) 1639–1643.

[8] H. Joshi, E. Topp, Hydration in hyaluronic acid and its esters using differential scanning calorimetry, Int. J. Pharm. 80 (1992) 213–225.

[9] K. Sung, E. Topp, Effect of drug hydrophilicity and membrane hydration on diffusion in hyaluronic acid ester membranes, J. Control. Release 37 (1995) 95–104.

[10] F. Artzner, R. Zantl, J.O. Rädler, Lipid–DNA and lipid–polyelectrolyte mesophases, structure and exchange kinetics, Cell. Mol. Biol. 46 (2000) 967–978.

[11] M. Ruponena, S. Ylä-Herttualab, A. Urttia, Interactions of polymeric and lyposomal gene delivery systems with extracellular glycosaminoglycans: physicochemical and transfection studies, Biochim. Biophys. Acta 1415 (1999) 331–341.

[12] D.W. Nitzan, U. Nitzan, P. Dan, S. Yedgar, The role of hyaluronic acid in protecting surface-active phospholipids from lysis by exogenous phospholipase, Rheumatology 40 (2001) 336–340.

[13] A. Herslof-Bjorling, L. Sunderlof, B. Porch, L. Valtcheva, S. Hjerten, Interaction of anionic polysaccharide and an oppositely charged surfactant, Langmuir 12 (1996) 4628–4637.

[14] E. Atkins, J. Sheehan, Hyaluronates: relations between molecular conformations, Science 179 (1973) 562–564.

[15] S. Lee, W. Oliver, A. Rupprecht, Z. Song, S. Lindsay, Observation of a phase transition in wet-spin films of Na hyaluronate, Biopolymers 32 (1992) 303–306.

[16] A. Mitra, S. Raghunathan, J. Sheehan, S. Arnott, Hyaluronic acid: molecular conformations and interactions in the orthorhombic and tetragonal forms containing sinuous chains, J. Mol. Biol. 169 (1983) 829–859.

[17] J. Sheehan, E. Atkins, X-ray fibre diffraction study of conformational changes in hyaluronate induced in presence of sodium, potassium and calcium cations, Int. J. Biol. Macromol. 5 (1983) 215–221.

[18] J. Sheehan, E. Atkins, I. Nieduszynski, X-ray diffraction study on the connective tissue polysaccharides, J. Mol. Biol. 91 (1975) 153–163.

[19] R. Ionov, A. El-Abed, A. Angelova, M. Goldmann, P. Peretti, Asymmetrical ion channel model inferred from two-dimensional

crystallization of peptide antibiotic, Biophys. J. 78 (2000) 3026–3035.

[20] M. Petty, Langmuir Blodgett Films—An Introduction, Cambridge University Press, Cambridge, 1996.

[21] T. Nakazawa, R. Azumi, H. Sakai, M. Abe, M. Matsumoto, Brewster angle microscopic observations of the Langmuir films of amphiphilic spiropyran during compression and under UV illumination, Langmuir 20 (2004) 5439–5444.

[22] J.M. Patino, M.C. Fernandez, Structural and topographical characteristics of adsorbed WPI and monoglyceride mixed monolayers at the air–water interface, Langmuir 20 (2004) 4515–4522.

[23] E. Loste, E. Díaz-Martí, A. Zarbakhsh, F.C. Meldrum, Study of calcium carbonate precipitation under a series of fatty acid Langmuir monolayers using Brewster angle microscopy, Langmuir 19 (2003) 2830–2837.

[24] R. Ionov, A. Angelova, Evidence for a discotic smectic–nematic phase induced in Langmuir–Blodgett films, Phys. Rev., E 52 (1995) R21–R25.

[25] R. Ionov, A. El-Abed, M. Goldmann, P. Peretti, Structural organization of α-helical peptide antibiotic alamethicin at the air/water interface, J. Phys. Chem., B 108 (2004) 8485–8488.

[26] A. El-Abed, R. Ionov, M. Goldmann, P. Fontaine, J. Billard, P. Peretti, Evidence for asymmetric edge-on Langmuir monolayer: application to surface potential measurements, Europhys. Lett. 56 (2001) 234–240.

[27] C. Fradin, J. Daillant, A. Braslau, D. Luzet, M. Alba, M. Goldmann, Microscopic measurement of the linear compressibilities of two-dimensional fatty acid mesophases, Eur. Phys. J., B Cond. Matter Phys. 1 (1998) 57–65.

[28] M. Jones, D. Chapman, Micelles, Monolayers and Biomembranes, Wiley-Liss, New York, 1995.

[29] A. Angelova, R. Ionov, Langmuir–Blodgett film organization resulting from asymmetrical or partial types of monolayer transfer: comparison for amphiphiles of different geometrical shapes, Langmuir 12 (1996) 5643–5653.

[30] K. Sung, E. Topp, Swelling properties of hyaluronic acid ester membranes, J. Membr. Sci. 92 (1994) 157–167.

[31] H.M. McConnell, L. Tamm, R. Weis, Fluorescence microscopy of Langmuir monolayers, Proc. Natl. Acad. Sci. U. S. A. 81 (1984) 3249–3254.

[32] R. Weis, H.M. McConnell, Observation of 2D domains in lipid monolayrs, Nature 310 (1984) 47–49.